

## Synthesis, characterization and catalytic CO oxidation studies over $\text{Ni}_{1-x}\text{Cu}_x\text{Mn}_2\text{O}_4$

S M Gurav & A V Salker\*

Department of Chemistry, Goa University, Goa 403 206, India

Received 15 June 1998; revised 2 September 1998

$\text{Ni}_{1-x}\text{Cu}_x\text{Mn}_2\text{O}_4$  ( $x = 0.0, 0.3, 0.5, 0.7, 1.0$ ) have been prepared by co-precipitation method and characterized by XRD, AAS and BET method. The solid state studies such as electrical resistivity, magnetic susceptibility and electron spin resonance (ESR) have been carried out and are attempted to correlate with the catalytic activity of the compounds. The model reaction of CO oxidation has been undertaken to evaluate the catalytic activity and kinetics. Higher activity of intermediate compositions is observed due to the phenomena of synergism.

Spinel shows interesting structural, electrical and magnetic properties besides catalytic applications<sup>1,2</sup>. Binary metal oxides especially those having spinel structure have been the subject of investigation with a view to their applications as substitutes for the noble metal containing catalysts for automobile and industrial purification of exhaust gases. CO oxidation has been studied over different types of catalysts by many investigators<sup>3,4</sup>. Studies have shown that as compared to individual oxides, spinel oxides are better catalysts on account of their activity and stability. The phenomenon of synergism in two metal based catalysts is a fascinating aspect in catalytic research. Presently, we report the electrical, magnetic and catalytic studies over  $\text{Ni}_{1-x}\text{Cu}_x\text{Mn}_2\text{O}_4$  synthesized by co-precipitation method.

### Materials and Methods

The compositions  $\text{Ni}_{1-x}\text{Cu}_x\text{Mn}_2\text{O}_4$  ( $x = 0.0, 0.3, 0.5, 0.7, 1.0$ ) were prepared by co-precipitation technique<sup>5</sup>. The required metal nitrates and acetates of AR grade were taken in stoichiometric proportions and dissolved in distilled water to obtain a clear homogeneous solution. To this, a solution of sodium hydroxide was added with constant stirring till the precipitation is complete. The precipitate thus obtained was digested on a water bath for 3 h. The precipitated hydroxides mixture was subjected to oxidation by dropwise addition of 30%  $\text{H}_2\text{O}_2$  from a burette with continuous stirring. The precipitate was then washed with water, filtered and dried at 353 K. The dried precipitate was homogenised well in a mortar and then

heated in a furnace at 973-1073 K for 10 h.

The compositions prepared by co-precipitation method were characterized by employing X-ray powder diffraction method (Philips XRD PW 1820) using  $\text{CuK}_\alpha$  and filtered through Ni absorber. The sodium contamination in the spinels prepared by co-precipitation method using NaOH, was found out using an Atomic Absorption Spectroscopy (AAS). Surface area of the compositions were measured using BET, nitrogen adsorption method (ANYGAS Version 2.10). Electrical conductivity measurements were carried by two probe conductivity cell in the temperature range of 300 - 723 K. The magnetic susceptibility ( $\chi_g$ ) in air of the spinels were determined by Guoy method at room temperature employing a field of the order of 10,000 gauss and using  $\{\text{Hg}[\text{Co}(\text{SCN})_4]\}$  as a standard material. The ESR spectra were taken at the X-band on a Varian E-112 spectrometer at  $298 \pm 2$  K at a field strength of 3220 gauss. The sample was mounted in a quartz tube and TCNE was used as a field calibrant taking its  $g$ -value as 2.00277. Spectroscopic splitting factor ( $g$ ) or gyromagnetic ratio was obtained from the relation  $\mu = -g\beta s$ , where ' $\mu$ ' is the magnetic moment, ' $\beta$ ' the Bohr magneton (ergs/gauss), ' $g$ ' the gyromagnetic ratio and ' $s$ ' is the spin of electron.

Oxidation of carbon monoxide by oxygen was studied in a continuous flow, fixed bed glass reactor, in which 1g of the catalyst powder was placed between glass wool plugs. The catalytic activity was determined using a feed gas composition of 5% CO, 5%  $\text{O}_2$  in nitrogen. The individual gas flow rates were

Table I—Kinetic parameters of CO oxidation over different catalysts

Catalysts	Surf. Area ( $\text{m}^2/\text{g}$ )	Temp ( $^\circ\text{K}$ )	Rate ( $\text{Molec.}/\text{m}^2.\text{s}$ )	$E_a$ ( $\text{kcal}/\text{mol}$ )	Freq. factor ( $\text{Molec.}/\text{m}^2.\text{s}$ )
$\text{NiMn}_2\text{O}_4$	5.6	512	$1.8 \times 10^{18}$	16.5	$1.8 \times 10^{18}$
$\text{Ni}_{0.7}\text{Cu}_{0.3}\text{Mn}_2\text{O}_4$	5.4	483	$2.3 \times 10^{18}$	12.2	$2.3 \times 10^{18}$
$\text{Ni}_{0.5}\text{Cu}_{0.5}\text{Mn}_2\text{O}_4$	3.2	440	$3.5 \times 10^{18}$	11.0	$3.5 \times 10^{18}$
$\text{Ni}_{0.3}\text{Cu}_{0.7}\text{Mn}_2\text{O}_4$	5.4	530	$2.36 \times 10^{18}$	13.7	$2.3 \times 10^{18}$
$\text{CuMn}_2\text{O}_4$	4.3	495	$2.20 \times 10^{18}$	12.6	$2.2 \times 10^{18}$

controlled using flow meters and precision needle valves. The feed gases and the products were analysed employing an on-line gas chromatograph with molecular sieve 13X column and  $\text{H}_2$  as a carrier gas. The CO was prepared by standard procedure and was purified by passing through appropriate traps. The nitrogen and oxygen gases were used from pure commercial cylinders.

### Results and Discussion

The samples prepared by co-precipitation were characterised by recording the X-ray diffractograms. The  $d_{hkl}$  and  $2\theta$  values obtained were compared with the values reported in the literature (JCPDS data file) and found to be monophasic. Since the  $d_{hkl}$  of the intermediate compositions are not reported in the literature, the values were compared with the end compositions.

Since sodium hydroxide was used in the preparation process, the sodium contamination was estimated using an AAS and was found to be in the range of 0.2% to 0.4% by weight. Surface areas obtained by using BET nitrogen adsorption method were found in the range of 3.20 to 5.60  $\text{m}^2/\text{g}$  for these compositions as shown in the Table 1.

On account of sensitivity of  $\text{CuMn}_2\text{O}_4$  to thermal treatment, one could not obtain a pure sample of this compound. Others<sup>6</sup> claim to have obtained it in a cubic phase and only Buhl<sup>7</sup> could synthesize it as a tetragonal phase by calcining at 1213 K and quenching from above 1023 K while below 1023 K,  $\text{CuMn}_2\text{O}_4$  progressively gets transformed into a cubic phase. Our results of X-ray analysis after comparison with the values reported in JCPDS data file has indicated that  $\text{CuMn}_2\text{O}_4$  and  $\text{NiMn}_2\text{O}_4$  are cubic spinels.

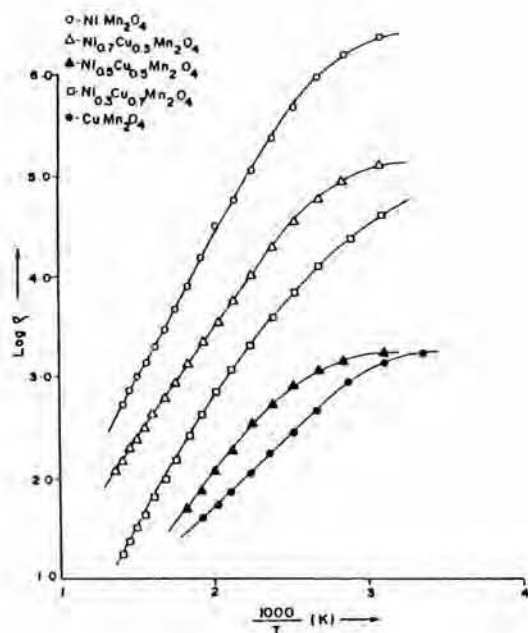
It is reported earlier<sup>8</sup> that  $\text{Cu}^{2+}$  has the strongest square ( $dsp^2$ ) bond forming power among metals of first transition series and is expected to occupy an octahedral site. Further, the results of an X-ray powder study by Zaslavskii *et al.*<sup>9</sup> showed that  $\text{CuMn}_2\text{O}_4$  is not a normal spinel but partially inverted with inversion parameter  $\lambda$  within the limits  $0.67 \leq \lambda \leq 1$ . Inverse structure of  $\text{NiMn}_2\text{O}_4$  from crystallographic data obtained by Sinha *et al.*<sup>10</sup> was supported by the fact that  $\text{Ni}^{2+}$  ions show strong tendency to occupy octahedral sites and suggested a structure as  $\text{Mn}^{2+}[\text{Ni}^{2+}\text{Mn}^{4+}]\text{O}_4^{2-}$ . In  $\text{Ni}_{1-x}\text{Cu}_x\text{Mn}_2\text{O}_4$ , symmetry is cubic throughout the system in accordance with the earlier reports<sup>6</sup>. The observed cubic symmetry over the entire range of composition is explained by Bhandage and Keer<sup>11</sup> as due to the absence of Jahn-Teller distortion on account of mutual neutralization of ions like  $\text{Cu}^{2+}$  and  $\text{Mn}^{3+}$  having tendency to distort the structure.

### Electrical resistivity

Electrical resistivity ( $\rho$ ) of these compounds were measured by two probe method from room temperature to 723 K. Plot of resistivity ( $\rho$ ) vs temperature (T) is shown in Fig. 1 for  $\text{Ni}_{1-x}\text{Cu}_x\text{Mn}_2\text{O}_4$ . Resistivity is found to decrease linearly with rise in temperature for all the compositions. Resistivity decreases with the increase in copper content in  $\text{Ni}_{1-x}\text{Cu}_x\text{Mn}_2\text{O}_4$  system. The improvement in conductivity is attributed to the copper content rather than nickel at a given temperature. From the literature it is seen that B-site cations are responsible for electrical conduction in spinels by virtue of symmetry. Thus more significant B-B interactions determine the electrical conduction, which is due to transfer of electrons from B-site  $\text{Mn}^{3+}$  ions to B-site  $\text{Mn}^{4+}$  ions<sup>2</sup>.

Table 2—Magnetic susceptibility and ESR data of different compositions

Catalysts	$\chi_g$	$\mu_{\text{eff}}$ (B.M)	g-Value	Line width (gauss)
NiMn <sub>2</sub> O <sub>4</sub>	$5.906 \times 10^{-5}$	5.7652	2.3288	1070
Ni <sub>0.7</sub> Cu <sub>0.3</sub> Mn <sub>2</sub> O <sub>4</sub>	$6.123 \times 10^{-5}$	5.8884	2.1173	800
Ni <sub>0.5</sub> Cu <sub>0.5</sub> Mn <sub>2</sub> O <sub>4</sub>	$5.637 \times 10^{-5}$	5.6615	1.9808	1484
Ni <sub>0.3</sub> Cu <sub>0.7</sub> Mn <sub>2</sub> O <sub>4</sub>	$5.785 \times 10^{-5}$	5.7472	1.9604	1950
CuMn <sub>2</sub> O <sub>4</sub>	$6.084 \times 10^{-5}$	5.9119	1.9570	780

Fig. 1—Variation of electrical resistivity of Ni<sub>1-x</sub>Cu<sub>x</sub>Mn<sub>2</sub>O<sub>4</sub> with temperature.

The electrical conductivity cannot be explained in copper manganite with ionic structure Cu<sup>2+</sup>[Mn<sub>2</sub><sup>3+</sup>]O<sub>4</sub><sup>2-</sup>, since electron cannot be transferred from Mn<sup>3+</sup> ion to another Mn<sup>3+</sup> ion. In Ni<sub>1-x</sub>Cu<sub>x</sub>Mn<sub>2</sub>O<sub>4</sub>, p-type conductivity was observed by many investigators for all the compositions except at x = 0. However, it is reported by Mulla and Darshane<sup>5</sup> that in NiMn<sub>2</sub>O<sub>4</sub>, when Mn<sup>3+</sup> < Mn<sup>4+</sup>, it exhibits n-type conductivity and when Mn<sup>3+</sup> > Mn<sup>4+</sup>, it is observed to be p-type. The conductivity in manganites could be explained on the basis of Mn<sup>4+</sup>-Mn<sup>3+</sup> ion pair association which is in agreement with reports given elsewhere<sup>12</sup>. The results can be easily explained on the basis of an electron transfer process shown elsewhere<sup>10</sup> as

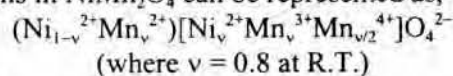


Higher resistivity observed for compositions with small x-value may be due to low concentration of Mn<sup>3+</sup>-Mn<sup>4+</sup> ion pairs resulting in the large average distance between equivalent sites available for hopping. With increase in copper content in solid solution, the number of Mn<sup>3+</sup>-Mn<sup>4+</sup> ion pairs, at B-site increases, resulting in the corresponding decrease of resistivity which is an inverse function of Mn<sup>4+</sup> ion concentration.

Nickel manganite is known to have cubic inverse spinel structure with Ni<sup>2+</sup> occupying octahedral B-site. Following are the ionic structures for NiMn<sub>2</sub>O<sub>4</sub> which are supported by many investigators<sup>2,13</sup>.

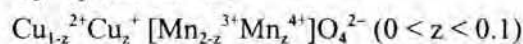


It is, however, reported elsewhere<sup>14</sup> that occupation of octahedral site by Ni<sup>2+</sup> reduces Mn<sup>3+</sup>/Mn<sup>4+</sup> redox couples on the same lattice site which are the cause for good electrical conductivity of nickel manganites. Mn<sup>2+</sup>[Ni<sup>2+</sup>Mn<sup>4+</sup>]O<sub>4</sub><sup>2-</sup> does not account for good electrical conductivity, which implies that a part of Ni<sup>2+</sup> cations may be in tetrahedral site. According to the recent studies carried out by Asbrinc<sup>15</sup>, the distribution of cations in NiMn<sub>2</sub>O<sub>4</sub> can be represented as,



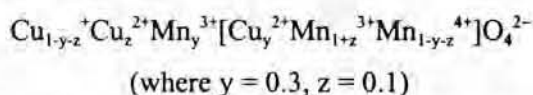
Thus the observed low conductivity in NiMn<sub>2</sub>O<sub>4</sub> could be explained as due to Mn<sup>3+</sup>-Mn<sup>4+</sup> ion pair association on the basis of above ionic distribution.

Higher conductivity of CuMn<sub>2</sub>O<sub>4</sub> can be attributed to the tetrahedrally located Cu<sup>2+</sup> and Cu<sup>1+</sup> ions besides Mn<sup>3+</sup>-Mn<sup>4+</sup> ion pairs which have been considered by some investigator<sup>6</sup>, with the ionic structure conventionally represented as,



Some others<sup>1</sup> have proposed the following configura-

ration for  $\text{CuMn}_2\text{O}_4$  based on structural, electrical and magnetic behaviour.



With the increase in  $x$ -value, resistivity is found to decrease for different compositions at a given temperature. Decrease in resistivity with increase in copper content is known due to  $\text{Mn}^{3+}\text{-Mn}^{4+}$  ion pairs.

#### Magnetic susceptibility

The magnetic susceptibility ( $\chi$ ) of different samples were determined by Guoy balance at room temperature employing a field strength of 10,000 gauss. The gram susceptibility values obtained at room temperature and their corresponding magnetic moments are presented in Table 2 for  $\text{Ni}_{1-x}\text{Cu}_x\text{Mn}_2\text{O}_4$  system.

Magnetic susceptibility for  $\text{NiMn}_2\text{O}_4$  is expected to be higher than that for  $\text{CuMn}_2\text{O}_4$ . However, the presence of  $\text{Cu}^{2+}$  and  $\text{Mn}^{3+}$  ions in the spinel which have substantial additional Jahn-teller stabilization on interaction results in the formation of ion pairs such as  $\text{Mn}^{3+}\text{-Mn}^{4+}$  along with  $\text{Cu}^{1+}$  or  $\text{Mn}^{3+}\text{-Mn}^{4+}$  with  $\text{Cu}^{1+}$  as well as  $\text{Cu}^{2+}$ . With increase in copper concentration in  $\text{Ni}_{1-x}\text{Cu}_x\text{Mn}_2\text{O}_4$ , B-B interaction becomes stronger with increasing  $\text{Mn}^{3+}\text{-Mn}^{4+}$  ion pairs, which facilitates the transfer of electrons thereby resulting in a increase of magnetic susceptibility. Formation of such  $\text{Mn}^{3+}\text{-Mn}^{4+}$  ion pairs raises the magnetic susceptibility which thus accounts for higher susceptibility value for  $\text{CuMn}_2\text{O}_4$ .

Among different compositions,  $\text{Ni}_{0.7}\text{Cu}_{0.3}\text{Mn}_2\text{O}_4$  exhibits highest magnetic susceptibility, which is on account of higher nickel content. Besides, the presence of little copper increases  $\text{Mn}^{3+}\text{-Mn}^{4+}$  ion pairs thus resulting in high overall magnetic gram susceptibility ( $6.123 \times 10^{-5}$ ). For  $\text{Ni}_{0.5}\text{Cu}_{0.5}\text{Mn}_2\text{O}_4$  composition, this effect is counterbalanced thus reducing the susceptibility value to its minimum (i.e.  $5.637 \times 10^{-5}$ ). Further increase in copper concentration (e.g.  $\text{Ni}_{0.3}\text{Cu}_{0.7}\text{Mn}_2\text{O}_4$ ) raises the susceptibility value to  $5.785 \times 10^{-5}$  which may be due to formation of a large number of  $\text{Mn}^{3+}\text{-Mn}^{4+}$  ion pairs along with  $\text{Ni}^{2+}$  ions. However, this value is comparatively smaller than that for  $\text{CuMn}_2\text{O}_4$  ( $6.084 \times 10^{-5}$ ) which is on account of added nickel.

The technique of ESR spectroscopy was used to get an insight of the catalytically active and paramag-

netic species such as  $\text{Cu}^{2+}$ . ESR data of different spinels is presented in Table 1. The  $g$ -value of ESR spectra for  $\text{Ni}_{1-x}\text{Cu}_x\text{Mn}_2\text{O}_4$  were gradually found to decrease with increase in  $x$ -value.

On account of strong octahedral site preference of  $\text{Cu}^{2+}$  ions it is expected to occupy B-site in  $\text{AB}_2\text{O}_4$  spinel system. Our results of ESR show that copper is the active species in which  $g$ -value observed for  $\text{CuMn}_2\text{O}_4$  is 1.9570 and for  $\text{NiMn}_2\text{O}_4$  it is 2.3288. The results are in consistent with the earlier reports<sup>11</sup> from which it is confirmed that nickel is present at B-site only and a part of  $\text{Cu}^{2+}$  ion occupies an octahedral site. The broadening of line width at  $x = 0.5$  and  $0.7$  may be due to several factors such as short spin relaxation time, spin-spin interaction, and structural configuration.

#### Catalytic oxidation of carbon monoxide

The temperature dependence of CO conversion studied over different compositions of  $\text{Ni}_{1-x}\text{Cu}_x\text{Mn}_2\text{O}_4$  is shown in Fig. 2. The rate of CO conversion increases with increase in ' $x$ ' and is maximum at  $x = 0.5$ , further increase in ' $x$ ' value declines the CO conversion rate. Thus  $\text{Ni}_{0.5}\text{Cu}_{0.5}\text{Mn}_2\text{O}_4$  exhibits relatively higher activity towards CO oxidation among the different compositions within the series. For arriving at any correlation between catalytic behaviour and other properties, the kinetic measurements of different compositions were carried out at low conversion rate and in the low temperature region. Fractional conversion of CO ( $X_{\text{CO}}$ ) versus  $W/F_{\text{CO}}$  where

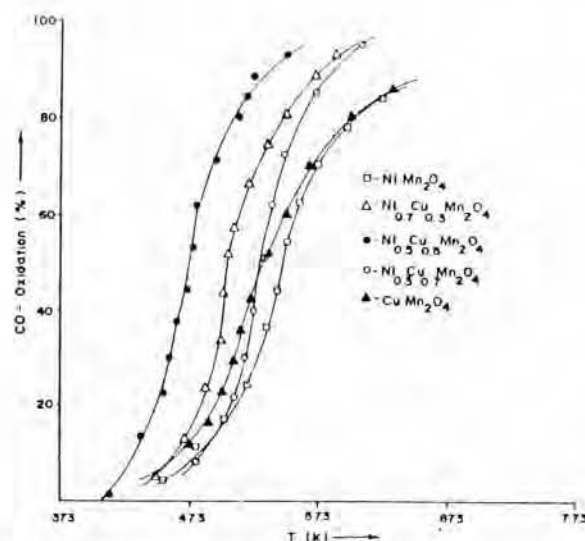


Fig. 2—CO conversion as a function of catalyst temperature for  $\text{Ni}_{1-x}\text{Cu}_x\text{Mn}_2\text{O}_4$ .

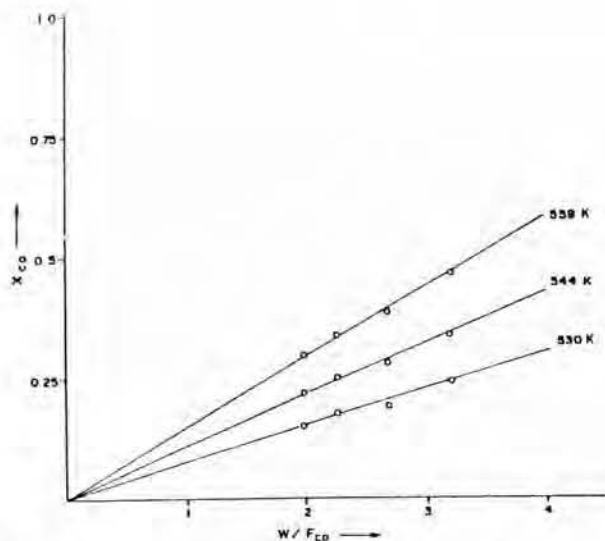


Fig. 3—Resident time plot for the representative sample of  $\text{Ni}_{0.3}\text{Cu}_{0.7}\text{Mn}_2\text{O}_4$ .

'W' is the mass of the catalyst taken and  $F_{\text{CO}}$  is the number of moles of CO flowing per hour, at different temperatures is shown for a representative sample in Fig. 3. Effect of change in composition on percentage conversion at different temperatures is shown in Fig. 4. The kinetic parameters such as the reaction rates, the activation energies ( $E_a$ ) and frequency factors (A) were evaluated from the Arrhenius plots and are summarised in Table 2.

In  $\text{Ni}_{1-x}\text{Cu}_x\text{Mn}_2\text{O}_4$ , composition with  $x = 0.5$  exhibits highest activity in terms of CO oxidation followed by  $0.3 > 0.7 > 1.0 > 0.0$ . The end compositions i.e.  $\text{NiMn}_2\text{O}_4$  and  $\text{CuMn}_2\text{O}_4$  showed lower activities. The CO conversion shown by intermediate compositions are relatively much higher than the end compositions. The higher activities can be attributed to the phenomena of synergism<sup>16</sup>, which results from the cooperative effect of two different metal ions i.e. nickel and copper in their divalent state placed on A-site of  $\text{AB}_2\text{O}_4$  spinel.

The trend in catalytic activity of intermediate compositions towards CO oxidation is quite difficult in the presence of three different metal ions, as large number of factors such as thermodynamic and kinetic parameters, site preference energies, preferential surface enrichment etc. play significant role in deciding the overall performance of such catalysts.

Some reports on mixed catalysts of manganese and copper have shown that at the surface of the catalyst copper ions are partially reduced by manganese ions

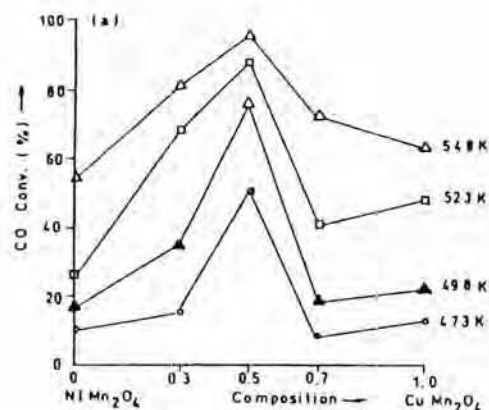


Fig. 4—Percentage conversion as a function of catalyst composition at different temperatures for the system  $\text{Ni}_{1-x}\text{Cu}_x\text{Mn}_2\text{O}_4$ .

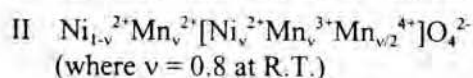
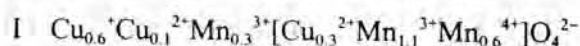
and this causes low activities of Mn containing mixed oxides<sup>17</sup>. However, partial replacement of copper by nickel creates a large number of  $\text{Ni}^{2+}$  and  $\text{Mn}^{4+}$  ions on the octahedral site due to their site preference energies, thus displacing  $\text{Mn}^{3+}$  ions to tetrahedral site, which is in agreement with earlier reports<sup>11</sup>.

The observed catalytic activity may be due to  $\text{Ni}^{2+}$  ions besides  $\text{Cu}^{2+}$  ions. Though copper is active in its dipositive oxidation state for CO oxidation, but unexpectedly the activity is found to be lower inspite of large copper content as observed for  $x = 0.7$ . This may be due to the surface enrichment of manganese over copper as reported elsewhere<sup>17</sup>. This also explains the low rate of CO oxidation over  $\text{CuMn}_2\text{O}_4$  compared to the intermediate compositions.

The low temperature CO conversion can be attributed to nickel rather than copper which is partly in its reduced state as  $\text{Cu}^{1+}$ . The presence of manganese which is constant throughout the series also affects the overall activity to some extent, since the presence of nickel and copper in different oxidation states gives rise to manganese species in oxidation state such as  $\text{Mn}^{2+}$ ,  $\text{Mn}^{3+}$  and  $\text{Mn}^{4+}$ . Therefore, though not significant, variable contribution of Mn ions towards CO oxidation for different compositions is also to be considered. The study reveals that it is a cooperative effect of two metals which gives pronounced change in CO conversion at  $x = 0.5$  at all the temperatures, thus indicating the typical phenomena of synergism which occurs by breaking the activation energy barrier of both limiting steps.

Our data of electrical resistivity, electron spin resonance and magnetic susceptibility are in agree-

ment with the ionic structures arrived earlier<sup>1,15</sup> for  $\text{CuMn}_2\text{O}_4$  and  $\text{NiMn}_2\text{O}_4$  respectively i.e.



On the bases of ionic structures, the catalytic oxidation of CO can be attributed to octahedrally placed  $\text{Cu}^{2+}$  species which are exposed exclusively at the surface of the spinel oxide as reported elsewhere<sup>18</sup> and that only these sites participates in reaction. Similarly CO conversion over  $\text{NiMn}_2\text{O}_4$  can be explained due to octahedrally exposed  $\text{Ni}^{2+}$  ions. In the ionic structure some of the copper ions ( $\text{Cu}^{2+}$ ) are also seen on the tetrahedral sites. Some of the investigators<sup>19</sup> have reported that activity of  $\text{Cu}^{2+}$  ions on tetrahedral site is more than octahedral sites on account of their large susceptibility for reduction. The above ionic structure explains the contribution of  $\text{Cu}^{2+}$  ions from tetrahedral site also towards CO oxidation. The presence of manganese in either of the oxidation states also helps to explain oxidation reaction via adsorption.

In  $\text{Ni}_{1-x}\text{Cu}_x\text{Mn}_2\text{O}_4$  system, the cubic symmetry is observed throughout the series in which the cooperative effect of two different A site metal ions (i.e.  $\text{Ni}^{2+}$  and  $\text{Cu}^{2+}$ ) results in the maximum catalytic activity at an intermediate composition of  $x=0.5$ . However for the compositions above and below  $x=0.5$  the activity falls down as shown in Fig. 4.

Activation energy for  $\text{Ni}_{0.5}\text{Cu}_{0.5}\text{Mn}_2\text{O}_4$  is found to be lowest i.e. 11.0 kcal/mol in this series with highest rate of reaction. Also the highest value of frequency factor explains the exposure of large number of active sites on the surface of the catalyst. The lowest frequency factor for  $\text{NiMn}_2\text{O}_4$  i.e.  $1.8 \times 10^{18}$  molec/ $\text{m}^2\text{s}$  with its low catalytic activity is attributed to nickel ions ( $\text{Ni}^{2+}$ ). Further, the improvement in the activity of  $\text{NiMn}_2\text{O}_4$  by addition of little quantity of copper indicates that the activity rise is due to available copper and nickel sites for the reaction. Approximately same frequency factor for composition with  $x = 0.3$  and 0.7 confirms that  $\text{Ni}^{2+}$  as well as  $\text{Cu}^{2+}$  ions participates in surface oxidation reaction. However, minor contribution from  $\text{Cu}^{1+}$ ,  $\text{Mn}^{2+}$ ,  $\text{Mn}^{3+}$  and  $\text{Mn}^{4+}$  cannot be neglected which could directly or indirectly affect the CO conversion.

## Conclusion

A significant rise in catalytic activity was observed by A-site substitution in the spinel  $\text{NiMn}_2\text{O}_4$ . CO oxidation on various catalyst compositions in the series showed that their end compositions are relatively less active than their intermediate compositions which is due to the phenomena of synergism. Composition with  $x = 0.5$  was found to exhibit maximum catalytic activity, may be due to large number of  $\text{Ni}^{2+}$  ions on octahedral site and  $\text{Cu}^{2+}$  on tetrahedral as well as octahedral sites available for reaction. Studies on electrical resistivity, electron spin resonance and magnetic susceptibility which were in agreement with the ionic structures arrived and site preference of metal ions helped in determination of catalytic activity towards CO oxidation.

## Acknowledgement

The authors are grateful to the CSIR, New Delhi, for the financial support.

## References

- 1 Bhandage G T & Keer H V, *J Phys C, Solid State Phys*, 8 (1975) 501.
- 2 Larson E G, Arnott R J & Wickham D G, *J Phys Chem Solids*, 23 (1962) 1771.
- 3 Tyurkin Yu V, Luzhkova E N, Pirogova G N & Chisalov L A, *Catal Today*, 33 (1997) 191.
- 4 Dekker F H M, Dekker M C, Bliet A, Kapteijn F, Moulijn J A, *Catal Today*, 20 (1994) 409.
- 5 Mulla B A & Darshane V S, *Indian J Chem*, 22A (1983) 143.
- 6 Kshirsagar S T, *J Phys Soc Japan*, 27 (1969) 1164.
- 7 Buhl R, *J Phys Chem Solids*, 30 (1969) 805.
- 8 Goodenough J B & Loeb A L, *Phys Rev*, 98 (1955) 398.
- 9 Zaslavskii A I, Karachentsva Z V & Zharinova A I, *Soviet Phys Crystallogr*, 7 (1963) 680.
- 10 Sinha A P B, Sanjana N R & Biswas A B, *Acta crystallogr*, 10 (1957) 439.
- 11 Bhandage G T & Keer H V, *J Phys C, Solid State Phys*, 9 (1976) 1325.
- 12 Ghare D B, Sinha A P B & Singh A L, *J Mat Sci*, 3 (1968) 389.
- 13 O'Keefe M, *J Phys Chem Solids*, 21 (1961) 172.
- 14 Laberty C, Verelst M, Lecante P, Alphonse P, Mosset A & Rousset A, *J Solid State Chem*, 129 (1997) 271.
- 15 Asbrinc S, Was'kawska A, Drozd M & Talik E, *J Phys Chem Solids*, 58 (1997) 785.
- 16 Laine J, Brito J, Severino F, Castro G, Tacconi P, Yunes S & Cruz J, *Catal Lett*, 5 (1990) 45.
- 17 Yang B L, Chan S F, Chang W S & Chen Y Z, *J Catal*, 130 (1991) 52.
- 18 Jacob J P, Matha A, Reintjes J G H, Drimal J, Ponec V & Brongersma H H, *J Catal*, 147 (1994) 294.
- 19 Ghose J & Murthy K S R C, *J Catal*, 162 (1996) 359.